Ultrastructure of the host–pathogen interface in *Arabidopsis thaliana* leaves infected by the downy mildew *Hyaloperonospora parasitica*

C.W. Mims, E.A. Richardson, B.F. Holt III, and J.L. Dangl

Abstract: Transmission electron microscopy was used to examine the host–pathogen interface in *Arabidopsis thaliana* (L.) Heynh. leaves infected by the biotrophic downy mildew pathogen *Hyaloperonospora parasitica* (Pers.:Fr.) Constant. Both conventionally fixed as well as high-pressure frozen samples were examined. Excellent preservation of the host–pathogen interface was obtained in many of our high-pressure frozen samples and provided information not available in conventionally fixed samples. Mature haustoria of *H. parasitica* were distinctly pyriform in shape. A small collar of host cell wall material surrounded the neck of each haustorium near the host cell wall penetration site. The presence of callose in collars was demonstrated using immunogold labeling with a monoclonal antibody specific for (1→3)-β-glucans. The body of each haustorium was ensheathed by an invaginated portion of the invaded host-cell plasma membrane known as the extrahaustorial membrane. Lying between this membrane and the haustorial wall was a layer of electron-dense material known as the extrahaustorial matrix (EHM). The EHM typically was thicker at the distal end of a haustorium than at the proximal end. The surface of the EHM covered by the extrahaustorial membrane was highly irregular in outline. Considerable vesicular activity was observed in association with the extrahaustorial membrane.

Key words: transmission electron microscopy, high-pressure freezing, haustoria, *Peronospora parasitica*.

Résumé : Les auteurs pont utilisé la microscopie électronique par transmission afin d'examiner l'interface hôte–pathogène, chez des feuilles de l'*Arabidopsis thaliana* (L.) Heynh. infectées par le champignon pathogène biotrophe du mildiou, l'*Hyaloperonospora parasitica* (Pers.:Fr.) Constant. Ils ont examiné des échantillons fixés par méthodes conventionnelles ainsi que congelés sous haute pression. On obtient ainsi une excellente conservation de l'interface hôte–pathogène, chez plusieurs des échantillons congelés sous haute pression, lesquels ont fourni des informations non disponibles par la voie conventionnelle. Les haustéries du *H. parasitica* apparaissent distinctement pyriformes. Un petit collier de matériel cellulaire de l'hôte entoure le col de chaque haustérie, près du point de pénétration de la paroi de la cellule hôte. On démontre la présence de callose dans les cols, en utilisant l'immuno-marquage à l'or avec l'anticorps monoclonal spécifique (1→3)-β-glucans. Le corps de chaque haustérie est entouré par une portion invaginée de la membrane plasmique de l'hôte, connue sous le nom de membrane extra-haustoriale. Entre cette membrane et la paroi de l'haustérie, on trouve une couche dense aux électrons connue sous le nom de matrice extra-haustoriale (EHM). La EHM est typiquement plus épaisse dans la partie distale de l'haustérie qu'à l'extrémité proximale. La surface de la EHM couverte par la membrane extra-haustoriale montre un contour fortement irrégulier. On observe une activité vésiculaire considérable en association avec la membrane extra-haustoriale.

Mots clés : microscopie électronique par transmission, fixation sous haute pression, haustérie, *Peronospora parasitica*.

[Traduit par la Rédaction]

Introduction

Since early descriptions of the *Arabidopsis thaliana* (L.) Heynh. – *Peronospora parasitica* (Pers.:Fr.) pathosystem (Koch and Slusarenko 1990; Holub et al. 1994; Holub and Beynon 1996), downy mildew disease of *A. thaliana* has become an extremely valuable model system for studying the interactions that occur between plants and pathogenic microorganisms (Slusarenko and Schlaich 2003; Takemoto et al. 2003). *Peronospora parasitica*, currently known as *Hyaloperonospora parasitica* (Pers.:Fr.) Constant., is a biotrophic oomycete that causes downy mildew disease of various Brassicaceae. However, there appears to be considerable host specificity among isolates of this pathogen (Holub and Beynon 1996), and those capable of infecting *A. thaliana* appear to be nonpathogenic to other plant species (Slusarenko and Schlaich 2003). In susceptible *A. thaliana* ecotypes, *H. parasitica* produces an extensive system of well-developed, aseptate, intercellular hyphae that give rise to numerous short branches known as haustoria that form

Received 6 October 2003. Published on the NRC Research Press Web site at http://canjbot.nrc.ca on 10 August 2004.

C.W. Mims.[1] Department of Plant Pathology, University of Georgia, Athens, GA 30602, USA.
E.A. Richardson. Department of Plant Biology, University of Georgia, Athens, GA 30602, USA.
B.F. Holt III and J.L. Dangl. Department of Biology, University of North Carolina, Chapel Hill, NC 27599, USA.

[1]Corresponding author (e-mail: cwmims@uga.edu).

 doi: 10.1139/B04-073

intimate relationships with living host cells (Koch and Slusarenko 1990; Parker et al. 1993; Donofrio and Delaney 2001; Soylu and Soylu 2003). Each haustorium breaches the host cell wall, but remains outside the physiological barrier of the invaded host cell by invaginating rather than penetrating the host-cell plasma membrane. As noted by Voegele and Mendgen (2003), haustoria are one of the hallmarks of true obligate biotrophic fungi and oomycetes. These structures long have been suspected of playing a role in nutrient absorption from invaded host cells, although this function has been difficult to document. Recently, however, there is growing evidence that haustoria function not only in nutrient absorption, but also in the suppression of host defense responses, in the redirection or reprogramming of the host's metabolic flow, and in biosynthesis (Voegele and Mendgen 2003).

Haustoria of a variety of biotrophic fungi and oomycetes have been studied at the ultrastructural level, some in great detail. Surprisingly, however, few studies focus on the haustoria of *H. parasitica*. Some data are available from a study of infected cabbage cotyledons conducted over 30 years ago (Chou 1970), and a few low-magnification views of haustoria formed in *A. thaliana* recently have been published by Soylu and Soylu (2003). As a result, we decided that it would be valuable to examine the ultrastructural features of the haustoria of this pathogen at high magnification in leaves of a susceptible ecotype of *A. thaliana*. For this study, we utilized the Emco5 isolate of *H. parasitica* propagated on the susceptible *A. thaliana* ecotype Wassilewskija (Ws-0) (Holub and Beynon 1996; McDowell et al. 1998). While we employed both conventional chemical fixation as well as high-pressure freezing – freeze substitution (HPF–FS) in this study, we were most interested in determining the value of the latter fixation technique for unveiling precise details of the host–pathogen interface in *A. thaliana* leaves infected by *H. parasitica*. To date HPF–FS has proven to be extremely valuable for transmission electron microscopic studies of host–pathogen interactions in plants infected by biotrophic fungal pathogens (Knauf et al. 1989; Mendgen et al. 1991; Mims et al. 2003; Celio et al. 2004). The data presented here are a prerequisite for future studies designed to explore ultrastructural details of incompatible reactions between *H. parasitica* isolates and *A. thaliana*.

Materials and methods

The Emco5 isolate of *H. parasitica* used in this study was maintained on susceptible *A. thaliana* plants as described by McDowell et al. (1998). The sporangia (commonly referred to in the literature as conidia) used as inoculum were obtained by briefly vortexing infected leaves bearing numerous external sporangiophores in distilled water. Ten-day-old Ws-0 plants were then sprayed with water containing 5×10^4 sporangia/mL, covered with clear plastic wrap, and placed in a growth chamber at 18–20 °C under short day length and approximately 100% relative humidity. At 4 d postinoculation leaf samples were excised from infected plants and prepared for study with transmission electron microscopy (TEM) using either a traditional chemical fixation procedure employing glutaraldehyde and OsO_4 (Taylor and Mims 1991) or HPF–FS. The procedures used for HPF–FS have been described in detail by Mims et al. (2003). Conventionally fixed samples were dehydrated and infiltrated with Spurr's resin, while a 1:1 mixture of Spurr's resin and Embed 812 was employed for HPF–FS samples. All samples eventually were embedded in resin using Nagle Contur Permanox disposable culture dishes as embedding molds. Following resin polymerization, culture-dish material was cut and peeled away from the resin to reveal a smooth resin surface that allowed us to examine embedded leaf samples by light microscopy. Using this procedure it was possible to locate and mark hyphae and haustoria inside leaf samples for subsequent thin sectioning for TEM. Sections were cut using an ultramicrotome equipped with a diamond knife, picked up on slot grids, and allowed to dry onto formvar-coated aluminum racks according to the procedures of Rowley and Moran (1975). Sections were poststained with uranyl acetate followed by lead citrate prior to examination with a Zeiss EM 902A microscope operating at 80kV.

Immunogold labeling was employed for the localization of callose in host cells invaded by haustoria. The antibody used was a monoclonal antibody recognizing (1→3)-β-glucans purchased from Biosupplies Australia Pty. Ltd. (Parkville, Victoria, Australia). A detailed description of procedures relating to the use of this antibody including control experiments can be found in Celio et al. (2004).

Results

The overall specimen quality obtained in our conventionally fixed samples (Figs. 1–3) was adequate for a general description of haustorium morphology in *H. parasitica* and for providing data relating to the overall spatial relationships between haustoria and host cells. However, these samples were not adequate for precise description of the host–pathogen interface in infected host cells. For this type of information, cryofixed samples (Figs. 4–14) were much more valuable, despite the fact that *A. thaliana* leaves proved to be very difficult to prepare for study using cryofixation. In most cases, only a few adequately preserved cells were found in most of the cryofixed leaf samples we examined. However, we did observe excellent preservation of the host–pathogen interface in these cells.

As evident in Fig. 1, the proximal end or neck region of a haustorium near the host cell wall penetration site was more narrow than the distal end, which terminated in an invaded mesophyll cell. Fully developed haustoria were conspicuously pyriform in shape and usually contained a large central vacuole (Fig. 4). In addition to vacuoles, each haustorium contained a typical complement of cellular organelles and inclusions including at least one nucleus as well as numerous mitochondria, Golgi bodies, and lipid droplets (Figs. 1, 4). Each haustorium was continuous with an intercellular hypha via a very highly constricted region at the penetration site (Figs. 1–3). The haustorial wall was continuous with, but slightly thinner than, the wall of its parent intercellular hypha (Figs. 1–3). A small collar of host cell wall material surrounded the proximal end of each haustorium near the penetration site (Figs. 1–4). This collar was slightly less electron dense than the remainder of the host cell wall, but did contain some small, irregularly shaped, electron-dense

Figs. 1–4. Transmission electron micrographs of conventionally fixed (1–3) and high-pressure frozen (4) samples of *Hyaloperonospora parasitica* haustoria in leaf cells of *Arabidopsis thaliana*. Fig.1. Near-median longitudinal section of a haustorium (H) showing its continuity with an intercellular hypha (ICH). Note the small collar of host cell wall material (C) associated with the haustorium. Other host-cell structures visible include the cell wall (asterisks), plastids (P) and the large central vacuole (HCV). Only a thin layer of host-cell cytoplasm (arrow) covers the distal end of the haustorium. Visible within the haustorium are a nucleus (N) as well as numerous mitochondria (M), lipid bodies (L), and vacuoles (V). The haustorium is ensheathed by an electron-dense layer of material known as the extrahaustorial matrix (arrowheads). Scale bar = 1 µm. Fig. 2. Higher magnification view of the penetration site from Fig. 1. The arrows show the continuity between the walls of the intercellular hypha (ICH) and the haustorium (H). Also visible are the collar (C) and a thin layer of electron-dense material (arrowheads) that separates the collar from the haustorial wall. This layer is continuous with the extrahaustorial matrix (EHM). The host cell wall is visible at the asterisks. Scale bar = 0.25 µm. Fig. 3. Example of a penetration site with a slightly larger collar (C) than shown in Fig. 2. Note the continuity of the walls (arrows) of the intercellular hypha (ICH) and haustorium (H), the electron-dense layer (arrowheads) continuous with the extrahaustorial matrix (EHM), and the host cell wall (asterisks). Scale bar = 0.25 µm. Fig. 4. Near median longitudinal section of a fully formed haustorium (H) from a cryofixed sample. Note the collar (C), extrahaustorial matrix (arrowheads), host-cell vacuole (HCV), and plastid (P). Visible in the haustorium are two nuclei (N), a large vacuole (V), extracted remains of lipid bodies (L), mitochondria (M), and a Golgi body (G). Scale bar = 1 µm.

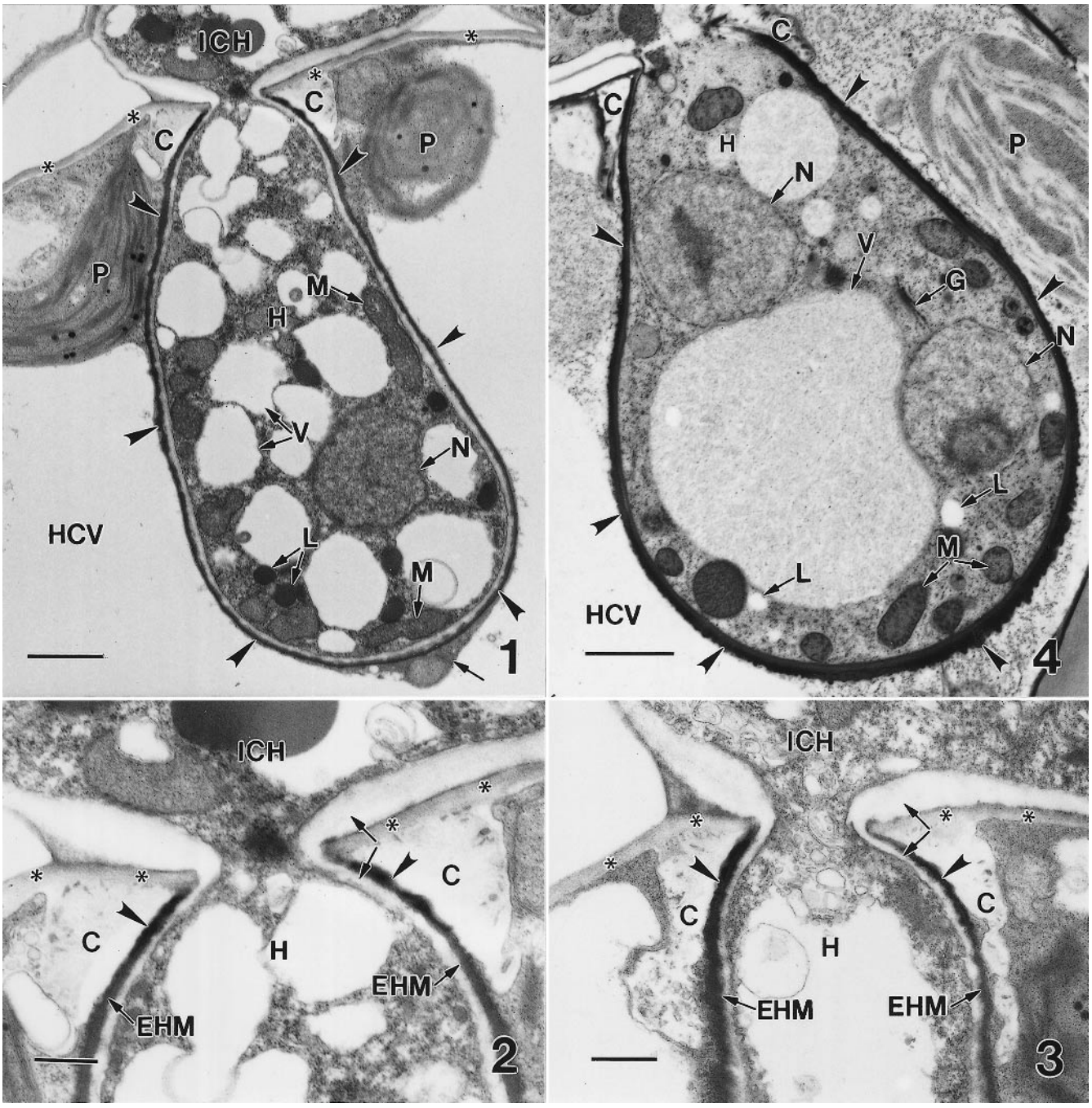

Figs. 5–9. Transmission electron micrographs of cryofixed samples of haustoria of *Hyaloperonospora parasitica* in leaf cells of *Arabidopsis thaliana*. Fig. 5. Immunogold labeling of a collar (C) with a monoclonal antibody recognizing (1→3)-β-glucan epitopes. Labeling of the wall of the intercellular hyphae (arrowhead) also occurred. The host cell wall is visible at the asterisks, and the invaginated host cell plasma membrane at PM. The thin layer of material that separates the collar from the haustorial wall is also evident at the arrow. Scale bar = 0.10 µm. Fig. 6. Gold labeling of the haustorial wall (HW) for (1→3)-β-glucans. The extrahaustorial matrix is visible at EHM. Scale bar = 0.10 µm. Fig. 7. High-magnification view of the interface between the distal end of a haustorium and a host cell. Visible are the haustorial plasma membrane (HM) and wall (HW), the extrahaustorial matrix (EHM), the extrahaustorial membrane (arrows), the tonoplast (T) of the host-cell vacuole (HCV), and numerous small vesicles (arrowheads) in the host-cell cytoplasm near the extrahaustorial membrane. Note the large protrusion of extrahaustorial matrix material (asterisk). Scale bar = 0.15 µm. Figs. 8, 9. Examples showing differences in the overall appearances of extrahaustorial matrix material (arrowheads) associated with the proximal ends of two haustoria. Also visible in each figure are the haustorial plasma membrane (HM) and wall (HW). A small vacuole (V), part of a mitochondrion (M), and a strand of rough endoplasmic reticulum (RER) are evident in the host-cell cytoplasm in Fig. 8. Scale bars = 0.30 µm.

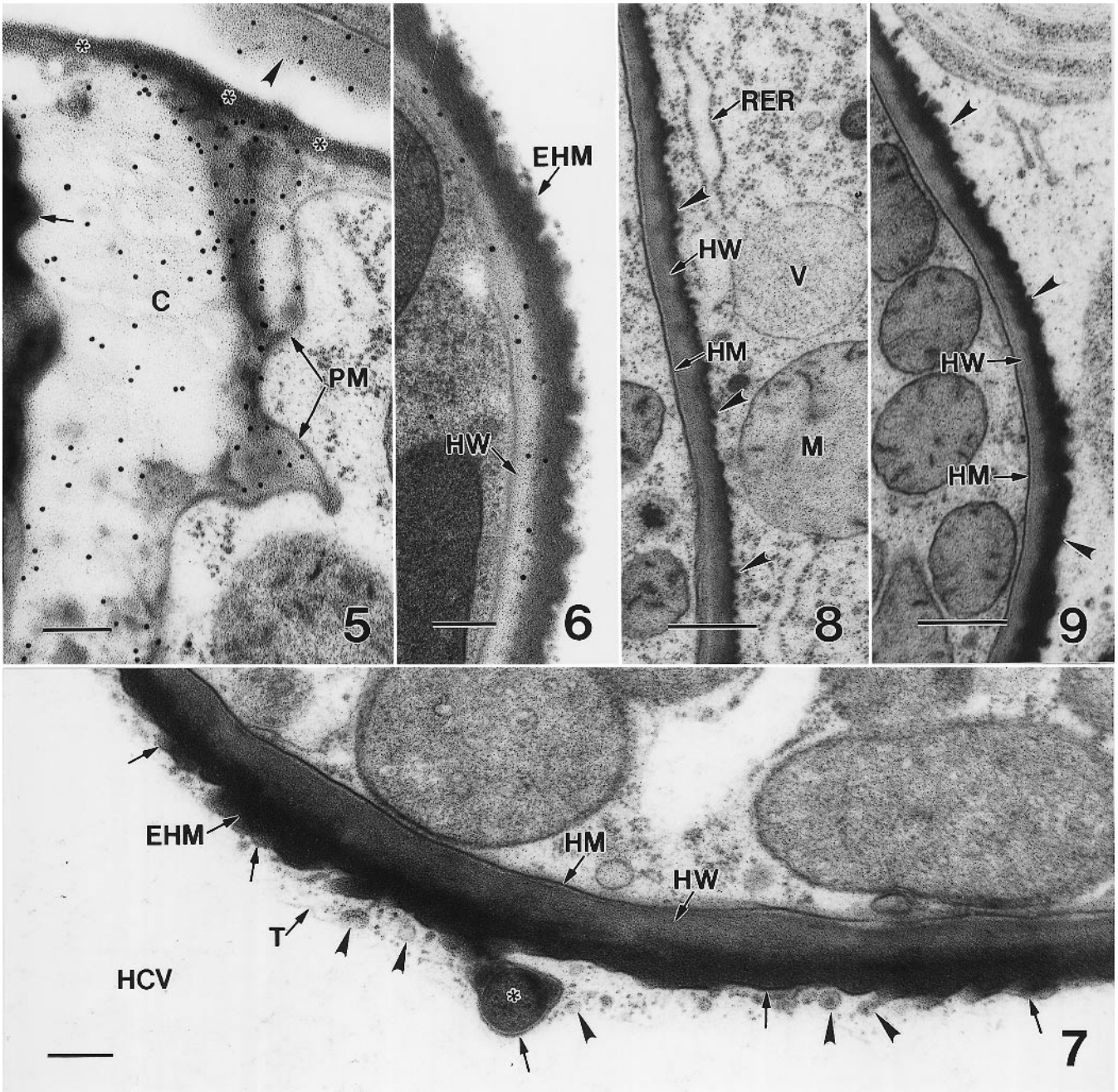

Figs. 10–14. Transmission electron micrographs of cryofixed samples of haustoria of *Hyaloperonospora parasitica* in leaf cells of *Arabidopsis thaliana*. Figs. 10–13. Examples of extrahaustorial matrix material (EHM) associated with four different haustoria. Note the less electron-dense nature of the EHM in Fig. 11 and a portion (asterisk) of the EHM in Fig. 10. The surface (arrows) of each EHM is highly irregular in outline. Note the tiny fingerlike projections of the EHM visible at the arrows in Fig. 13. Scale bars = 0.3 μm. Fig. 14. Example of a vesicle (arrow) in close association with the extrahaustorial matrix (EHM). Scale bar = 0.15 μm.

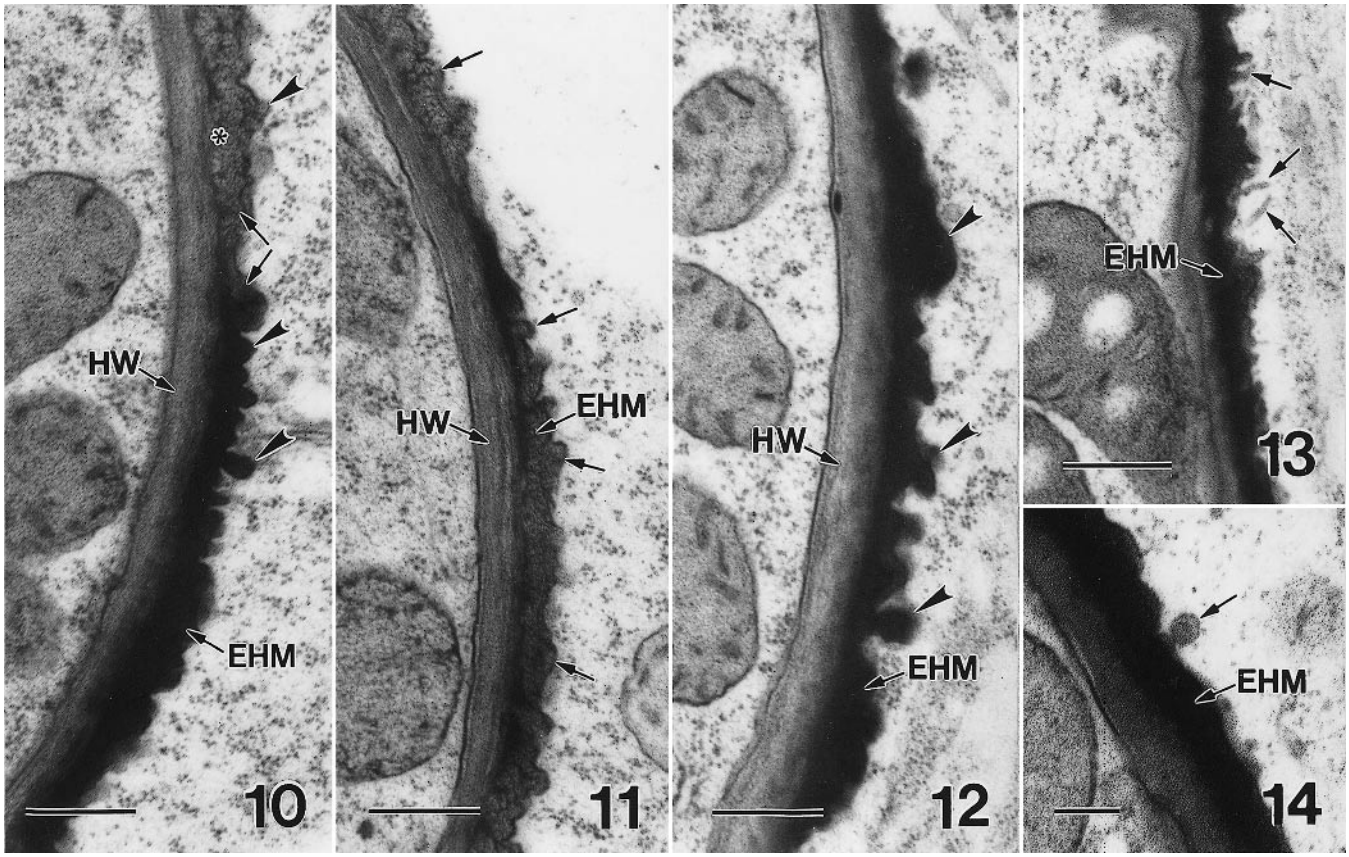

inclusions (Fig. 1–3). Collars could be labeled with an antibody specific for (1→3)-β-glucans, indicating the presence of callose (Fig. 5). This antibody also labeled (1→3)-β-glucans in the walls of both intercellular hyphae (Fig. 5) and haustoria (Fig. 6) of *H. parasitica*.

A thin layer of very electron-dense material separated the haustorial wall from the collar of host cell wall material (Figs. 2, 3, 5). This layer was continuous with a slightly less electron-dense layer of material (Figs. 2, 3) known as the extrahaustorial matrix (EHM) that ensheathed the wall of each haustorium (Figs. 1, 2). Separating the outer surface of the EHM from the host-cell cytoplasm was an invaginated portion of the host-cell membrane known as the extrahaustorial membrane (Figs. 7, 11). Because of the large central vacuole that typically filled most of the volume of a host mesophyll cell, the distal end of a haustorium typically was surrounded by only a very thin layer of host-cell cytoplasm sandwiched between the extrahaustorial membrane and the tonoplast of the host-cell vacuole (Figs. 1, 7).

The EHM typically was thicker at the distal end of a haustorium (Fig. 4, 7) than at the proximal end (Figs. 2, 8, 9). In a few cases, the EHM at the proximal end of a haustorium was extremely thin (Fig. 8). The bulk of the EHM associated with a haustorium was quite electron dense and exhibited little evidence of substructure (Figs. 7, 9). However, slightly less electron-dense regions of the EHM that exhibited a slightly fibrillar substructure were also observed (Figs. 10, 11). The outer surface of the EHM covered by the extrahaustorial membrane was highly irregular in outline (Figs. 6–13). In addition to possessing rounded protrusions of various sizes (Figs. 7, 10–12), the EHM surface sometimes possessed tiny fingerlike protrusions (Fig. 13). We also observed many small vesicles in the host-cell cytoplasm very near the extrahaustorial membrane (Fig. 7). Some of these vesicles appeared to be in the process of either fusing with or blebbing off the extrahaustorial membrane (Figs. 7, 14).

The haustorial wall was considerably less electron dense than the EHM (Figs. 8–13) and was of fairly uniform thickness over the entire surface of a haustorium. In cryofixed samples, the plasma membrane of each haustorium was closely appressed to the haustorial wall and exhibited a very smooth profile (Fig. 7–9).

Discussion

This study provides the first high-magnification views of the haustoria of the downy mildew pathogen *H. parasitica* produced in a susceptible ecotype of *A. thaliana* and represents the first report of the use of HPF–FS to study details of

the host–pathogen interface in any oomycete-incited plant disease. While the overall quality of data we collected using HPF–FS fixation was superior to that obtained from our conventionally fixed samples, the technique was particularly robust. *Arabidopsis* leaves proved to be very difficult to freeze, and only a few well-preserved cells per leaf samples were obtained. As a result, we expended a considerable amount of time and effort sectioning cryofixed samples to identify these cells. However, the excellent preservation of details of the host–pathogen interface in the rare, well-preserved cells justified our efforts. As reported in other studies (Knauf et al. 1989; Mendgen et al. 1991; Mims et al. 2003; Celio et al. 2004), HPF–FS is clearly the gold standard for studying details of the EHM and extrahaustorial membrane.

Haustorium morphology is one of the characteristics used in defining the newly erected genus *Hyaloperonospora*. As noted by Constantinescu and Fatehi (2002), members of this genus possess globose to lobate haustoria, while species of *Peronospora* have hyphal-like haustoria. Haustoria of stains of *H. parasitica* are clearly of the globose type. The extremely pyriform appearance of the mature haustoria of *H. parasitica* we observed in *Arabidopsis* cells agrees closely with light microscopic observations of these structures (Koch and Slusarenko1990; Soylu and Soylu 2003). Additionally, Chou (1970) described the haustoria of *H. parasitica* produced in cabbage cotyledons as being pyriform in shape. This is in contrast to the more elongated and hyphal-like haustoria reported for various species of *Peronospora* (Hickey and Coffey 1977; Beakes et al. 1982; Trigiano et al. 1983; Williamson et al. 1995).

The small cell wall deposits or collars we observed in association with haustoria of *H. parasitica* have been demonstrated previously in infected *A. thaliana* leaves using both light microscopy and TEM (Koch and Slusarenko1990; Nishimura et al. 2003; Soylu and Soylu 2003). It appears that these collars (sometimes referred to as papillae) correspond to the small structures that fluoresce blue when infected *A. thaliana* leaves are treated with analine blue and examined under ultraviolet light. The positive labeling of collars with an antibody recognizing (1→3)-β-glucans provides further evidence of the presence of callose in collars produced in *A. thaliana.* The labeling of the walls of both the intercellular hyphae and haustoria of *H. parasitica* reflects the fact that (1→3)-β-glucans are present in hyphal walls of oomycetes (Peberdy 1990).

Callose deposition by *A. thaliana* in response to invasion by *H. parasitica* has been demonstrated in numerous studies. Parker et al. (1993) reported that restriction of hyphal growth during incompatible host–pathogen reactions was accompanied by what was termed massive callose accumulations, while Donofrio and Delaney (2001) described four types of interactions in a detailed study that examined the growth and development of *H. parasitica* in susceptible wild-type as well as in defense-compromised strains of *A. thaliana*. In one type of reaction, no callose deposits were observed in response to haustoria, while in a second type, callose deposition was limited to narrow collars associated with haustorial necks. The latter phenotype is consistent with our observations. The two other types of reactions noted by Donofrio and Delaney (2001) involved rather massive encasements of haustoria by callose deposits. Interestingly, a recent study by Nishimura et al. (2003) demonstrated that disruptions in a callose synthase gene in *A. thaliana* eliminated accumulation of (1→3)-β-glucans in papillae, but led to a phenotype with increased resistance to several pathogens including *H. parasitica* and the powdery mildew fungi *Erysiphe cichoraceaum* and *Erysiphe orontii*. These papillae appear intact and might be interesting subjects for further ultrastructural studies of the *H. parasitica* – *A. thaliana* interface.

We believe that the thin layer of electron-dense material present between a collar and the wall of a haustorium of *H. parasitica* (Figs. 2 and 3) is a remnant of the so-called penetration matrix that has been reported in a number of oomycete-incited plant diseases, including downy mildew of cabbage (Chou 1970) and pea (Hickey and Coffey 1977; Beakes et al. 1982), blue mold of tobacco (Trigiano et al. 1983), late blight of potato (Coffey and Wilson 1983), and *Phytophthora* root rot of soybean (Enkerli et al. 1997). A penetration matrix initially appears as a very electron-dense deposit lying between the host cell wall and plasma membrane at a penetration site. Once the host cell wall has been penetrated by the pathogen, the penetration matrix appears to spread over the surface of the developing haustorium as it grows into the host-cell lumen by invaginating the host-cell plasma membrane (Chou 1970; Hickey and Coffey 1977). The penetration matrix appears to develop into or at least become continuous with the EHM that coats the haustorium. The remnant of the penetration matrix that persists at the penetration site appears to completely seal the space between the haustorium wall and the collar. This material may help prevent the flow of materials between the haustorial wall and collar and out of the host cell at the penetration site. If so, this layer of material may be analogous to neckbands that have been described in the haustoria of both rust (Heath 1976; Harder and Chong 1991) and powdery mildew fungi (Bracker 1968). A neckband is an electron-dense deposit in the wall of the neck of a haustorium that appears to seal the fungal plasma membrane with the invaginated host-cell plasma membrane. These structures have been compared with Casparian strips in plants (Heath 1976) and are thought to prevent the apoplastic escape of materials from the extrahaustorial matrix surrounding a haustorium, which might be regarded as a symplastic compartment (Heath and Skalamera 1997). Interestingly, neckbands have not been reported in association with oomycete haustoria.

Examination of the host–pathogen interface in *A. thaliana* leaves infected with downy mildew revealed some differences between the details of this interface and those found in rust and powdery mildew infections. First of all, the bulk of the EHM associated with the haustoria of *H. parasitica* was much more electron dense than the EHM typically found in association with either rust (Harder and Chong 1991; Knauf et al. 1989; Mims et al. 2001, 2002) or powdery mildew haustoria (Bracker 1968; Hippe 1985; Celio et al. 2004). Secondly, the outer surface of the EHM in infected *A. thaliana* cells was much more highly convoluted than that in rust infections. The highly convoluted nature of the EHM in oomycete-incited diseases appears to be quite common and has been demonstrated previously in downy mildew infections by Chou (1970), Hickey and Coffey (1977), and

Beakes et al. (1982). Thirdly, unlike the situation in rust and powdery mildew infections, the extrahaustorial membrane in infected *A. thaliana* cells was not significantly different in appearance from a typical plant-cell plasma membrane. This is in contrast to the situation in powdery mildew infections in which the extrahaustorial membrane has been shown to be significantly thicker than the host-cell plasma membrane (Bracker 1968; Gil and Gay 1977; Celio et al. 2004) and in rust infections in which the extrahaustorial membrane has been often shown to be continuous with prominent membranous elements that extend out into the surrounding host-cell cytoplasm (Harder and Chong 1991; Mims et al. 2001, 2002).

Voegele and Mendgen (2003) recently have suggested that the EHM likely plays a key role in the maintenance of the biotrophic lifestyle and is the site for the exchange of information and nutrients between host and pathogen. The highly irregular features of the outer surface of the EHM we observed in the current study coupled with the apparent vesicular activity noted in the host-cell cytoplasm very near the extrahaustorial membrane support the idea that the interface between the EHM and the extrahaustorial membrane is a very active site.

Future ultrastructural studies of the host–pathogen interface in a variety of incompatible reactions between *H. parasitica* and *A. thaliana* mediated by different *RPP* disease resistance gene products will contribute to a better understanding of the nature of this host–pathogen interface. In particular, we would like to assess how *Arabidopsis* defense-signaling mutants might alter the host–pathogen interface and how polarization of the host cell and directional delivery of vacuolar contents to the site of infection is mediated upon successful recognition of *H. parasitica* (Gross et al. 1993; Collins et al. 2003).

References

Beakes, G.W., Singh, H., and Dickinson, C.H. 1982. Ultrastructure of the host–pathogen interface of *Peronospora viciae* in cultivars of pea which show different susceptibilities. Plant Pathol. **31**: 343–354.

Bracker, C.E. 1968. Ultrastructure of the haustorial apparatus of *Erysiphe graminis* and its relationship to the epidermal cell of barley. Phytopathology, **58**: 12–30.

Celio, G.J., Richardson, E.A., and Mims, C.W. 2004. Ultrastructure and immunocytochemistry of the host–pathogen interface in poinsettia leaves infected with powdery mildew. Can. J. Bot. **82**: 421–429.

Chou, C.K. 1970. An electron-microscope study of host penetration and early stages of haustorium formation of *Peronospora parasitica* (Fr.) Tul. on cabbage cotyledons. Ann. Bot. (Lond.), **34**: 189–204.

Coffey, M.D., and Wilson, U.E. 1983. An ultrastructural study of the late-blight fungus *Phytophthora infestans* and its interaction with the foliage of two potato cultivars possessing different levels of general (field) resistance. Can. J. Bot. **61**: 2669–2685.

Collins, N.C., Thordal-Christensen, H., Lipka, V., Bau, S., Kombrinks, E., Qui, J.-L., Huckelhoven, R., Steins, M., Freialdenhoven, A., Somerville, S.C., and Schulze-Lefert, P. 2003. SNARE-protein-mediated disease resistance at the plant cell wall. Nature (Lond.), **425**: 973–977.

Constantinescu, O., and Fatehi, J. 2002. *Peronospora*-like fungi (Chromista, Peronosporales) parasitic on Brassicaceae and related hosts. Nova Hedwigia, **74**: 291–338.

Donofrio, N.M., and Delaney, T.P. 2001. Abnormal callose response phenotype and hypersusceptibility to *Peronospora parasitica* in defense compromised *Arabidopsis* nim1-1 and salicylate hydroxylase-expressing plants. Mol. Plant–Microbe Interact. **14**: 439–450.

Enkerli, K., Hahn, M.G., and Mims, C.W. 1997. Ultrastructure of compatible and incompatible interactions of soybean roots infected with the plant pathogenic oomycete *Phytophthora sojae*. Can. J. Bot. **75**: 1493–1508.

Gil, F., and Gay, J.L. 1977. Ultrastructure and physiological properties of the host interfacial components of haustoria of *Erysiphe pisi* in vivo and in vitro. Physiol. Plant Pathol. **10**: 1–12.

Gross, P., Julius, C., Schmelzer, E., and Hahlbrock, K. 1993. Translocation of cytoplasm and nucleus to fungal penetration sites is associated with depolymerization of microtubules and defense gene activation in infected, cultured barley cells. EMBO J. **12**: 1738–1744.

Harder, D.E., and Chong, J. 1991. Rust haustoria. *In* Electron microscopy of plant pathogens. *Edited by* K. Mendgen and D.-E. Lesemann. Springer-Verlag, Berlin. pp. 235–250.

Heath, M.C. 1976. Ultrastructural and functional similarity of the haustorial neckband of rust fungi and the Casparian strip of vascular plants. Can. J. Bot. **54**: 2484–2489.

Heath, M.C., and Skalamera, D. 1997. Cellular interactions between plants and biotrophic fungal parasites. Adv. Bot. Res. **24**: 195–225.

Hickey, E.L., and Coffey, M.D. 1977. A fine-structural study of the pea downy mildew fungus *Peronospora pisi* and its host *Pisum sativum*. Can. J. Bot. **55**: 2845–2858.

Hippe, S. 1985. Ultrastructure of *Erysiphe graminis* f. sp. *hordei* preserved by freeze substitution. Protoplasma, **129**: 52–61.

Holub, E.B., and Beynon, J.L. 1996. Symbiology of mouse ear cress (*Arabidopsis thaliana*) and oomycetes. Adv. Bot. Res. **24**: 228–273.

Holub, E.B., Beynon, J.L., and Crute, I.R. 1994. Phenotypic and genotypic characterization of interactions between isolates of *Peronospora parasitica* and accessions of *Arabidopsis thaliana*. Mol. Plant–Microbe Interact. **7**: 223–239.

Koch, E., and Slusarenko, A. 1990. *Arabidopsis* is susceptible to infection by a downy mildew fungus. Plant Cell, **2**: 437–445.

Knauf, G.M., Welter, K., Mullër, M., and Mendgen, K. 1989. The haustorial host–parasite interface in rust infected bean leaves after high pressure freezing. Physiol. Mol. Plant Pathol. **34**: 519–530.

McDowell, J.M., Dhandaydham, M., Long, T.A., Aarts, M.G.M., Goff, S., Holub, E.B., and Dangl, J.L. 1998. Intragenic recombination and diversifying selection contribute to the evolution of downy mildew resistance at the RPP8 locus of Arabidopsis. Plant Cell, **10**: 1861–1874.

Mendgen, K., Welter, K., Scheffold, F., and Knauf-Beiter, G. 1991. High pressure freezing of rust infected leaves. *In* Electron microscopy of plant pathogens. *Edited by* K. Mendgen and D.-E. Lesseman. Springer-Verlag, Berlin. pp. 31–42.

Mims, C.W., Rodriguez-Lother, C., and Richardson, E.A. 2001. Ultrastructure of the host–pathogen interaction in leaves of *Duchesnea indica* infected by the rust fungus *Frommeëla mexicana* var. *indicae* as revealed by high pressure freezing. Can. J. Bot. **79**: 49–57.

Mims, C.W., Rodriguez-Lother, C., and Richardson, E.A. 2002. Ultrastructure of the host–pathogen interface in daylily leaves

infected by the rust fungus *Puccinia hemerocallidis*. Can. J. Bot. **219**: 221–226.

Mims, C.W., Celio, G.J., and Richardson, E.A. 2003. The use of high pressure freezing to study host–pathogen interactions in fungal diseases of plants. Microsc. Microanal. **9**: 522–531.

Nishimura, M.T., Stein, M., Hou, B.-H., Vogel, J.P., Edwards, H., and Somerville, S. 2003. Loss of callose synthase results in salicylic acid-dependent disease resistance. Science (Washington, D.C.), **301**: 967–972.

Parker, J.E., Szabo, V., Staskawicz, B.J., Lister, C., Dean, C., Daniels, M.J., and Jones, J.D.G. 1993. Phenotypic characterization and molecular mapping of the *Arabidopsis thaliana* locus RPPP5, determining disease resistance to *Peronospora parasitica*. Plant J. **4**: 821–831.

Peberdy, J.F.1990. Fungal cell walls: a review. *In* Biochemistry of cell wall and membranes in fungi. *Edited by* P.J. Kuhn, A.P.J. Trinci, M.W. Goosey, and C.G. Copping. Springer-Verlag, Berlin. pp. 5–30.

Rowley, C.R., and Moran, D.T. 1975. A simple procedure for mounting wrinkle-free sections on formvar-coated slot grids. Ultramicroscopy, **1**: 151–155.

Slusarenko, A.J., and Schlaich, N.L. 2003. Downy mildew of *Aradidopsis thaliana* caused by *Hyaloperonospora parasitica* (formerly *Peronospora parasitica*). Mol. Plant Pathol. **4**: 159–170.

Soylu, E.M., and Soylu, S. 2003. Light and electron microscopy of the compatible interaction between *Arabidiopsis* and the downy mildew pathogen *Peronospora parasitica*. J. Phytopathol. **151**: 300–306.

Takemoto, D., Jones, D.A., and Hardham, A.R. 2003. GFP-tagging of cell components reveals the dynamics of subcellular reorganization in response to infection of *Arabidopsis* by oomycete pathogens. Plant J. **33**: 775–792.

Taylor, J., and Mims, C.W. 1991. Fungal development and host cell responses to the rust fungus *Puccinia substriata* var. *indica* in seedlings and mature leaves of susceptible and resistant pearl millet. Can. J. Bot. **69**: 1207–1219.

Trigiano, R.N., Van Dyke, C.G., and Spurr, H.W, Jr. 1983. Haustorial development of *Peronospora tabacina* infecting *Nicotiana tabacum*. Can. J. Bot. **61**: 3444–3453.

Voegele, R.T., and Mendgen, K. 2003. Rust haustoria: nutrient uptake and beyond. New Phytol. **159**: 93–100.

Williamson, B., Breese, W.A., and Shattock, R.C. 1995. A histological study of downy mildew (*Peronospora rubi*) infection of leaves and developing fruits of tummelberry and other *Rubus* spp. Mycol. Res. **99**: 1311–1316.